Denoising in Mode Conversion by Utilizing Diffractive Deep Neural Networks Optimized with Reinforcement Learning

Zheng Li[1,#], Wenbo Zhang[1,#], Yang Wang[1], Guanju Peng[1,*], Zongze Li[2,*], Xiaoyan Zhou[1,2], Lin Zhang[1,2,*]

[1]*Key Laboratory of Opto-electronic Information Technology of Ministry of Education and Tianjin Key Laboratory of Integrated Opto-electronics Technologies and Devices, School of Precision Instruments and Opto-electronics Engineering, Tianjin University, Tianjin, 300072, China*

[2]*Peng Cheng Laboratory, Shenzhen 518038, China*

**Corresponding author: guanjup@tju.edu.cn, lizz@pcl.ac.cn, lin_zhang@tju.edu.cn*

Abstract: We propose a reinforcement-learning-optimized nonlinear physical diffractive neural network, which can simultaneously perform OAM-mode and LP-mode conversion with Gaussian noise removal. The PSNR and SSIM of the converted modes reach 27.94 dB and 0.838, respectively.

1. Introduction

Optical fibers have emerged as a pivotal technology in modern communications, enabling long-haul high-bandwidth data transmission [1-3]. Few-mode fibers typically support a few guided modes, and each mode is characterized by a distinct distribution of light intensity and phase over the cross-section of the fiber [4]. The methods to efficiently control and convert these guided modes are vital to various applications, from fiber-based sensors to high-capacity data transmission systems. Early devices for mode conversion, including mode converters and mode multiplexers are often complex, bulky, and expensive [5,6]. The recently emerging artificial intelligence techniques have provided novel solutions to various complex problems in optics [7-9]. In particular, diffractive deep neural networks (D^2NN) [10], which have all-optical machine learning framework by harnessing the principles of wave propagation and interference, have shown great potential in addressing intricate optical tasks, including the mode conversion.

Pioneering work on all-optical D^2NNs machine learning framework shows the deep learning methods to design successive diffractive layers that are physically fabricated to perform statistical inference based on a trained task [10]. However, most D^2NNs only achieve image-to-label tasks, e.g., image classification, by setting several specific areas on the output plane as image category labels [11,12]. Although D^2NN can reconstruct images, it is still an open question that how much the reconstructed image quality can be improved using D^2NN.

Here, we build a new all-optical D^2NN, named nonlinear physical diffractive neural network (NPDNN), which can simultaneously transform 6 LP-mode profiles and 3 orbital angular momentum (OAM) [5] mode profiles to each other. While accomplishing mode conversion, the proposed NPDNN can significantly reduce the speckle effects induced by Gaussian noise. In the absence of noise, the NPDNN achieves a mode conversion with a peak signal-to-noise ratio (PSNR) [13] of 31.84 dB, a structural similarity index (SSIM) [14] of 0.897 and a learned perceptual image patch similarity (LPIPS) [15] of 0.074. When Gaussian noise becomes strong with a mean and standard deviation both less than 0.5 added, the NPDNN still achieves remarkable mode conversion results with a slightly smaller PSNR of 27.94 dB, an SSIM of 0.838 and an LPIPS of 0.143.

2. NPDNN configuration, results of mode conversion and mode denoising

We form a deep Q-learning (DQN) optimized 3D-printed NPDNN for multifunctional mode conversion, as shown

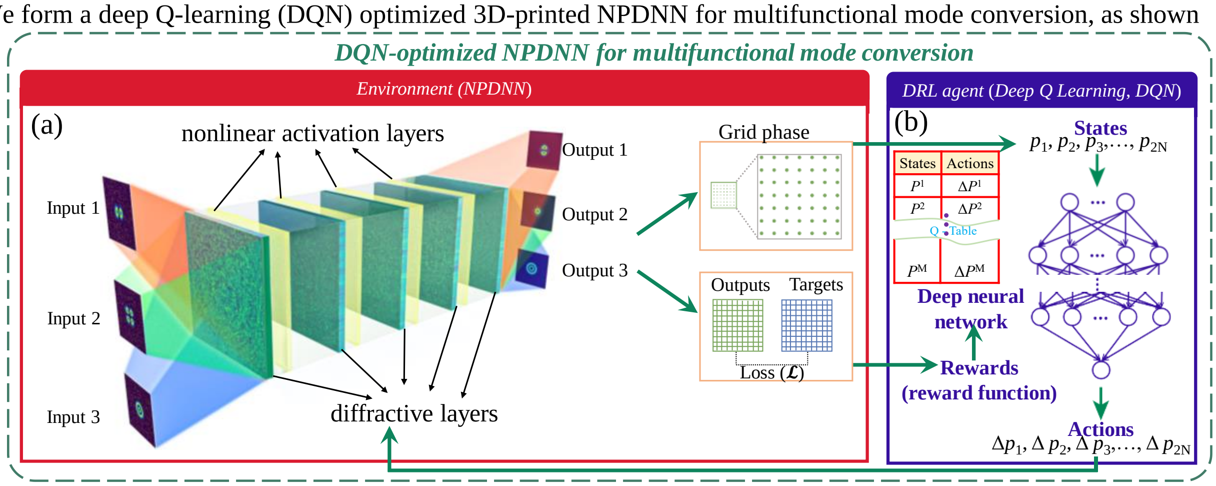

Fig. 1. Schematic of DQN-optimized NPDNN for multifunctional mode conversion. (a) An example was to reconstruct 3 modes (Denoising in mode conversion of the LP_{11a}, LP_{21b}, and OAM_1 modes to the LP_{11b}, LP_{01}, and OAM_2 modes, respectively) using NPDNN. (b) DQN reinforcement learning algorithm for optimizing NPDNN.

#: These two authors contributed equally to this work.

Our datasets and results will be released publicly at: https://github.com/zhemglee/NPDNN_LGOAM in Fig. 1. To verify the effectiveness of the NPDNN, we utilize the NPDNN conversion of three input modes to the corresponding three output modes first. For all studies in this paper, the NPDNN we constructed comprises 5 diffractive layers of phase plates at an incident wavelength of 1.55 μm. These phase plates are spaced 30 mm apart from each other, and following nonlinear function layer after each plate. Each phase plate has the size of 80 mm×80 mm and is further divided into 256×256 cells. In the DQN optimization step, the phase of each cell is the hyperparameter, and the NPDNN serves as the optimization environment to interact with the DQN agent. Meanwhile the rewards, states, and actions of the DQN agent are loss function ($\boldsymbol{\mathcal{L}}$), phases of all cells, and changes of phase in NPDNN, respectively.

To train the NPDNN to achieve multifunctional 9-mode conversion by leveraging the NPDNN, we create a dataset comprising 13000 data samples, encompassing 9 different modes, including 6 LP-modes (LP_{01}, $LP11_a$, $LP11_b$, LP_{21a}, LP_{21b}, and LP_{02}) and 3 OAM-modes (OAM_1, OAM_2, and OAM_3). In typical optical fiber communication systems, noise is introduced by mode generator, which results in input modes experiencing varying degrees of noise. To mitigate Gaussian noise $N(\mu, \sigma^2)$ effects, we set noise with different (μ, σ^2) of fiber modes in the dataset to investigate the performance of the NPDNN on denoising in conjunction with multifunctional mode conversion. This dataset is divided into 10000 samples as the training set and the rest 3000 samples as the test set. The training set includes input modes and target modes as data pairs, as shown in Fig. 2.

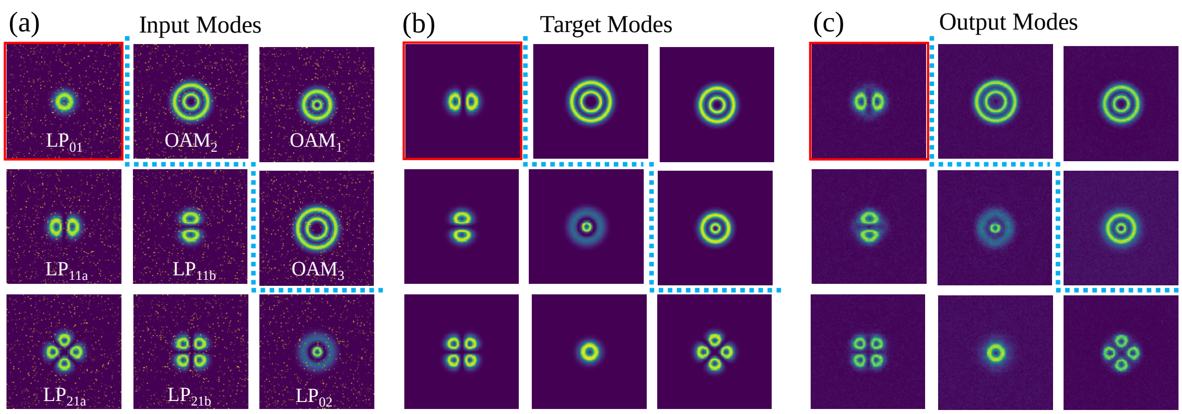

Fig. 2. Dataset description. (a) The 9 input modes with certain Gaussian noise. (b) The noiseless 9 target modes. The input modes and the target modes are the data pairs used for training. For example, the LP_{01} mode within the red box in Fig. 2(a) is transformed into the corresponding LP_{11a} mode within the red box in Fig. 2(b) by using the NPDNN. (c) In the absence of target modes in the test set, the mode conversion and denoising for the input modes are produced simultaneously by the trained NPDNN.

Our objective is to transform the input modes into the target modes, and the NPDNN enables to achieve perfect conversion for every detail and pixel of modes. Compared to the tasks of image classification, our task places significantly higher demands, particularly requiring it to possess nonlinear expressive capabilities. Consequently, we introduce two types of nonlinear activation functions [17,18] with the capability of nonlinear phase modulation as nonlinear activation layers placed after each diffractive layer. These two functions can achieve nonlinear activation functions like Tanh and Relu, named as OTanh and ORelu in optical domain, respectively. The performance is shown in Fig. 3(a). The loss function for the training process is defined as the sum of $\boldsymbol{\mathcal{L}}_2$, $\boldsymbol{\mathcal{L}}_{MS\_SSIM}$, and $\boldsymbol{\mathcal{L}}_{FSIM}$ (Please

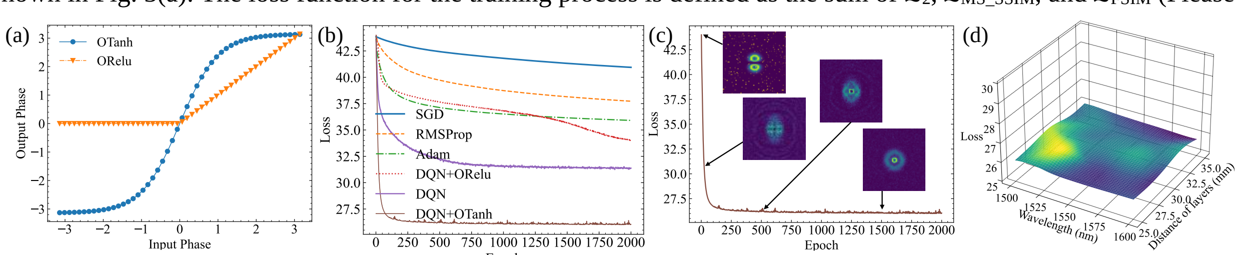

Fig. 3. (a) Two types of all-optically nonlinear activation functions. (b) For multifunctional 9-mode conversion by NPDNN, the loss ($\boldsymbol{\mathcal{L}}$) over epoch is shown by different algorithms. Compared to other algorithms, the DQN algorithm with the OTanh nonlinear layers has the fastest convergence speed and the minimum loss. (c) In the case of DQN+OTanh, the LP_{11b} mode with Gaussian noise of $N(0.5, 0.5^2)$ gradually evolves into the noiseless LP_{02} mode as the epoch increases. (d) 3D distribution of the loss with respect to wavelength and exponent of different distance.

Table 1: Loss terms ablation studies.

Loss Terms ~ $N(0.5, 0.5^2)$	PSNR ↑	SSIM ↑	LPIPS ↓
\ (Input-Target)	16.80	0.588	0.362
$\mathcal{L}_1$	18.14	0.789	0.265
$\mathcal{L}_2$	19.08	<u>0.830</u>	0.237
$\mathcal{L}_2$+$\mathcal{L}_{MS\_SSIM}$	<u>21.12</u>	0.821	<u>0.140</u>
$\mathcal{L}_2$+$\mathcal{L}_{FSIM}$	20.38	0.824	0.178
$\mathcal{L}_2$+$\mathcal{L}_{MS\_SSIM}$+$\mathcal{L}_{FSIM}$	**27.94**	**0.838**	**0.113**

Table 2: Image metric indicators under different noise levels.

Gaussian Nosise	PSNR ↑		SSIM ↑		LPIPS ↓	
Noise Levels	In-Tar	Out-Tar	In-Tar	Out-Tar	In-Tar	Out-Tar
$N(0.0, 0.0^2)$	16.91	**31.84**	0.807	**0.897**	0.196	**0.074**
$N(0.0, 0.5^2)$	14.14	27.41	0.786	0.840	0.282	<u>0.088</u>
$N(0.5, 0.0^2)$	15.90	<u>29.52</u>	0.797	<u>0.864</u>	0.256	0.097
$N(0.5, 0.5^2)$	14.80	27.94	0.788	0.838	0.362	0.143
$N(0.0, 1.0^2)$	8.68	22.75	0.485	0.609	0.663	0.385

(* The "↑" represents that a higher value is better for the corresponding metric indicators (also apply to "↓")).

refer to [16] for the details). The impact of different algorithms and nonlinear layers on the loss function is compared (SGD, Adam, and RMSProp), and the results are shown in Fig. 3(b). In addition, LP_{11b} mode gradually evolves into LP_{02} mode as the epoch increases, are shown in Fig. 3(c). Fig. 3(d) shows that the loss of NPDNN is insensitive to wavelength and distance of layers, making it easy to optimize and manufacture.

We have conducted ablation studies on the loss function, as shown in Table 1. The maximum and second maximum values for each metric are indicated by a bold and an underline font, respectively (also apply to Table 2). Our loss functions for PSNR, SSIM, and LPIPS have the best measurement results. In Table 2, we provide a summary of PSNR, SSIM, and LPIPS at different noise intensities. The "In-Tar" and "Out-Tar" in Table 2 represent indicator measurement results of the input modes and output modes with target modes, respectively. In addition, we demonstrate the mode conversion performance of LP_{21a} and OAM_2 modes at different noise levels, as shown in Fig. 4. It is evident that even in the presence of strong noise in input modes, the trained NPDNN can still achieve mode conversion and mode denoising simultaneously, with the PSNR of output modes more than 20 dB.

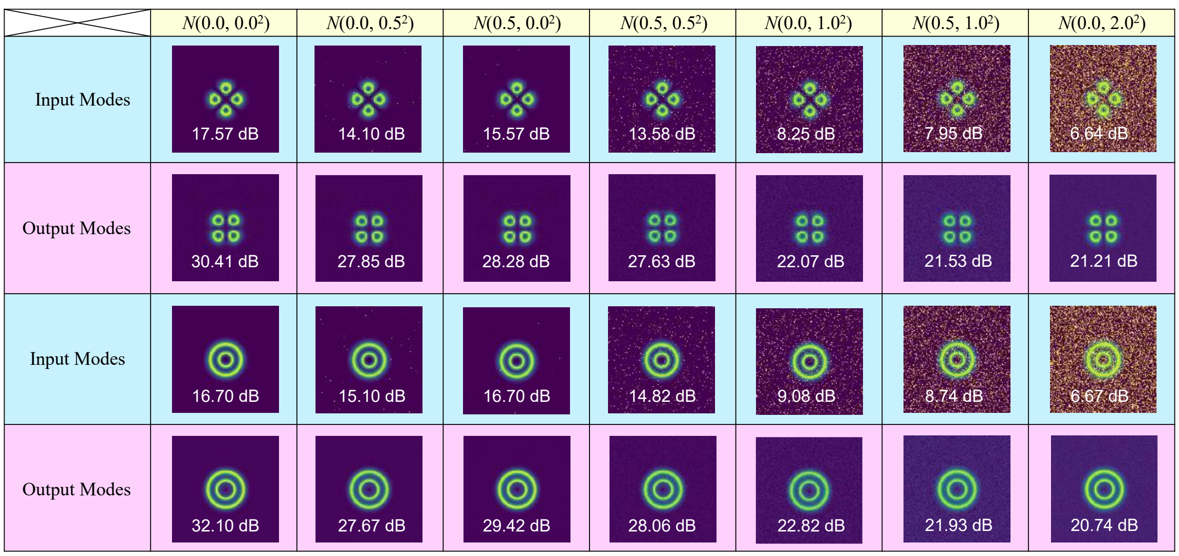

Fig. 4. Mode conversion of the LP_{21a} mode and the OAM_2 mode to the LP_{21b} mode and the OAM_3 mode, as examples respectively, under different noise levels. The values of the evaluator PSNR are given.

3. Conclusion

We have proposed a DQN-optimized nonlinear physical diffractive neural network, which can simultaneously perform multifunctional mode conversion and denoising. The simulations show that, when the noise coefficient is less than 0.5, the PSNR, SSIM, and LPIPS can reach 27.94 dB, 0.838, and 0.143, respectively. The outcomes of our proposed NPDNN have the potential to pave the way for greatly improving mode manipulations, leading to more efficient and high-quality optical communications.

References

[1] H. Wen, et al. *JLT*, 2016, **34**: 1990-96.
[2] G. Li, et al. *AOP*, 2014, **6**: 413–87.
[3] W. Ren, et al. *Optik*, 2016, **127**: 3248-52.
[4] Y. Zhang, et al. *JLT*, 2020, **38**: 6286-91.
[5] H. Wen, et al. *PR*, 2021, **9**: 88-97.
[6] N.K. Fontaine, et al. *NC*, 2019, **10**: 1865.
[7] X. Lin, et al. *Science*, 2018, **36**: 1004-8.
[8] H. Dou, et al. *OL*, 2020, **45**: 2688-91.
[9] Y. Qu, et al. *OL*, 2023, **48**: 5025-28.
[10] C. He, et al. *OEA*, 2024, **7**: 1-9.
[11] M. Lou, et al. *OL*, 2023, **48**: 219-22.
[12] O. Kulce, et al. *LSA*, 2021, **10**: 1-17.
[13] Y. Huang, et al. *TMM*, 2019, **21**: 2447-60.
[14] Z. Wang, et al. *TIP*, 2014, **13**: 600-12.
[15] R. Zhang, et al. in 2022 *CVPR*, 18311777.
[16] L. Zhang, et al. *TIP*, 2011, **20**: 2378-86.
[17] F.Z. Henari, et al. in 2014 *APMAS*, 020044.
[18] C. Dong, et al. *OLT*, 2023, **160**: 109104.